



Quasi-Steady Numerical Approach to Investigated Intake Starting and Unstart

Andreas K. Flock¹, Adrian T.E. Krieger², Ali Gülhan³
German Aerospace Center (DLR), Germany

Abstract

In all sorts of Ramjet engines the intake serves as the major component to compress the flow to sufficiently large pressures. With its location being far upstream, its performance is crucial for all following components such as combustor or nozzle. One major physical effect that influences intake performance is intake starting and unstart. During intake unstart, the shock system within the diffuser quickly moves upstream and mass flow and thus thrust are reduced. Therefore, a proper understanding of the unstart and then re-start behavior is essential for a correct operation of the engine. This manuscript presents a numerical, quasi-steady approach to duplicate the starting and unstart characteristics with a CFD approach. An axisymmetric intake configuration was used as reference configuration. In small steps the free stream Mach number is decreased and then again increased while intake performance is monitored. Furthermore, the starting and unstart characteristics were extracted from wind tunnel experiments. When comparing an initially unstarted, but then accelerated intake to an initially started, but decelerated intake, a hysteresis effect was present: The intake unstart occurred at lower free stream Mach numbers than the restart. This hysteresis effect was also detected during the wind tunnel experiments. Overall, the re-start and unstart Mach numbers, detected with the numerical approach were within 7 % of the values detected during experiment.

Keywords: *Ramjet, Diffuser, Supersonic*

Nomenclature

Latin

A – Area, m²
 $C1$ – Empirical constant
 CR – Contraction ratio
 M, Ma – Mach number
 $p0$ – Total pressure, bar
 q – Dynamic pressure, bar
 r – Radius, m
 Re – Reynolds number
 T – Temperature, K
 $T0$ – Total temperature, K
 x, y, z – Spatial coordinates, m

Greek

γ – Ratio of specific heats

Superscripts

* – Critical condition

Subscripts

∞ – Free stream
 c – Cone
 cl – Cowl closure
 i – Internal
 st – Static
 th – Throat
 w – Wall

¹Research Scientist, Launch Systems Department, German Space Agency, Königswinterer Str. 522, 53227 Bonn, Germany, e-mail: andreas.flock@dlr.de

²Research Scientist, Transport and Propulsion Systems Department, Institute of Space Systems, Robert-Hooke-Str. 7, 28359 Bremen, Germany

³Department Head, Supersonic and Hypersonic Technologies Department, Institute of Aerodynamics and Flow Technology, Linder Höhe, 51147 Cologne, Germany

1. Introduction

Air breathing engines use the surrounding air as oxidizer to power a vehicle. Therefore, their efficiency is usually better compared to conventional rocket engines. In the supersonic and hypersonic regime the ram effect becomes sufficient for compression. Thus, so called Ramjet engines become the natural extension of the jet engines for large velocities. Their technology readiness level is still lower, compared to their competitors - rocket engines. Furthermore, there are still active research programs focused on several fundamentals, components, or subsystems.

One such component is the air intake, which serves as the compressor of the air breathing power cycle. Compared to a conventional compressor the intake appears mechanically and geometrically simple, due to the lack of complex moving parts, such as rotating machinery. Nevertheless, it reveals interesting and complex flow phenomena. Examples are aerodynamic heating, laminar-turbulent boundary layer transition, or intake starting and unstart with hysteresis effects. Furthermore, with its location being far upstream its performance is directly influencing all following components such as the combustion chamber and nozzle. Therefore, the intake is a very crucial component for a successful operation of a ramjet engine.

The present paper investigates the already mentioned intake starting and unstart effects. The so called Kantrowitz diagram (figure 1) was frequently used by previous researchers [13, 8, 3, 16] to better understand and quantify intake starting. Within the diagram, the Kantrowitz limit,

$$CR_{\text{Kantrowitz}} = \frac{A_{\text{cl}}}{A_{\text{th}}} = \left(\frac{(\gamma + 1)M_{\text{cl}}^2}{(\gamma - 1)M_{\text{cl}}^2 + 2} \right)^{0.5} \left(\frac{(\gamma + 1)M_{\text{cl}}^2}{2\gamma M_{\text{cl}}^2 - (\gamma - 1)} \right)^{\frac{1}{\gamma - 1}}, \quad (1)$$

and the isentropic limit,

$$CR_{\text{isentropic}} = \frac{A_{\text{cl}}}{A_{\text{th}}} = \frac{1}{M_{\text{cl}}} \left[\frac{2}{\gamma + 1} \left(1 + \frac{\gamma - 1}{2} M_{\text{cl}}^2 \right) \right]^{\frac{\gamma + 1}{2(\gamma - 1)}}, \quad (2)$$

form three regions of interest: First, for $CR_i < CR_{\text{Kantrowitz}}$, a region in which intakes are always self-starting according to Kantrowitz. Second, for $CR_i > CR_{\text{isentropic}}$, a region in which intakes do not work properly as they are always unstarted. Third, a critical region in between, where intakes can generally work once successfully started. Equation (1) and (2) are theoretical approximations and only give a guideline for the restart and unstart limit. Therefore, a proper knowledge of the transition region from start to unstart and vice versa has to be obtained by other means.

Several authors proposed polynomial equations, to quantify the transition region [16, 15]. Their approximations are based on the general trends observed in experimental data. Furthermore, an adjustable equation was derived in [4] (see eq. (6) therein) that can be varied with a constant and that is shown for $C1 = 1.8$ in figure 1. Finally, a semi-empirical relation is shown, which was derived by modifying Kantrowitz' underlying assumptions. More precisely, the losses in total pressure, which were modeled by a normal shock in Kantrowitz' theory, were replaced with the losses of a strong oblique shock. Further information and a detailed derivation can be found in [4].

In the past years, different numerical approaches to study intake starting phenomena have been proposed and investigated. For example, the usage of a diaphragm was proposed and studied numerically in Euler [17, 18] and RANS simulations [12]. Furthermore, variable geometry and thus overboard spillage was studied, which allowed for an increase and decrease of internal contraction ratio [1, 6, 12]. Two-dimensional and three-dimensional geometries were compared [5], and the influence of backpressure was studied numerically [7, 9]. Further reading, about a review of numerical starting techniques can be found in [10, pp.26]. All of these numerical studies have in common, that they perform transient simulations to capture the behavior of starting and unstart.

In contrast to other authors, this manuscript presents a quasi-steady approach to determine the unstart and restart characteristics of an axisymmetric intake configuration. Next, a detailed description of the intake model, its characteristics and of the numerical approach are given. The results, first, give a

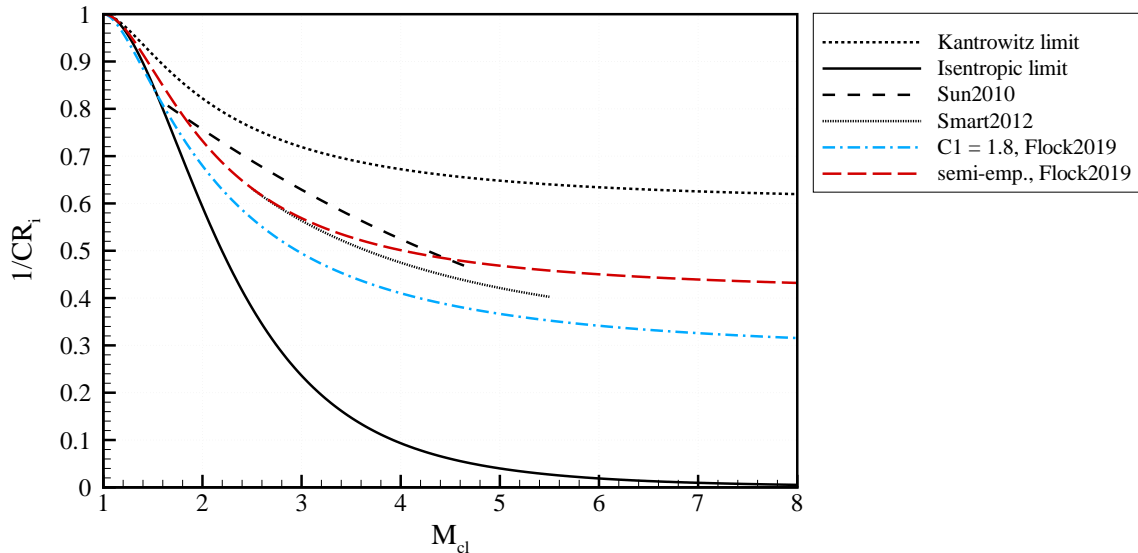


Fig 1. The Kantrowitz diagram: internal contraction ratio plotted against Mach number at cowl closure.

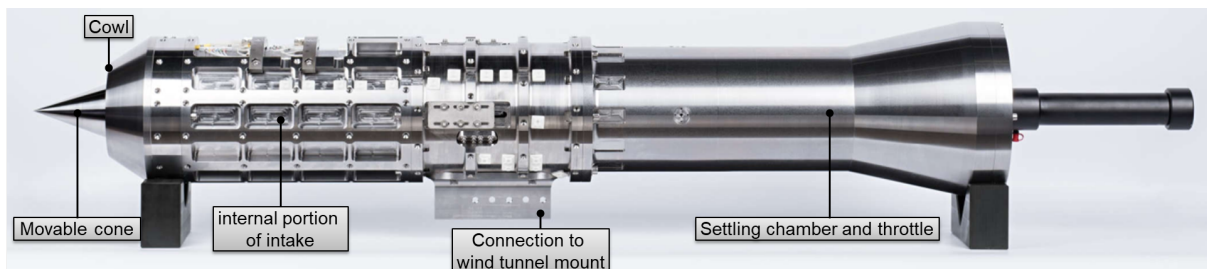


Fig 2. Image of the intake model for wind tunnel testing.

general discussion of the intake flow field. Second, the experimental data with regard to intake re-start and blockage is analyzed. And finally, the numerical results are compared to the experimental outcome.

2. Methods and Materials

2.1. Axisymmetric Intake Model

An axisymmetric intake model with a 20 deg cone was used as reference configuration. A wind tunnel model (see figure 2) was designed, to also investigate the configuration experimentally. One core feature of the intake model is the movable cone, which could be shifted in axial direction.

Figure 3 shows a sketch of the axisymmetric configuration, and the surrounding numerical domain. For the numerical simulations, the intake was cut off downstream of the throat, and did not contain the following settling chamber and throttle. As mentioned before, the cone location x_c could be shifted, and thus also the cross sectional area at the cowl closure A_{cl} and throat A_{th} could be varied. Figure 4 shows several features of the axisymmetric intake, plotted against cone-location. It can be concluded that: First, the internal contraction ratio decreases when the cone is moved upstream until $x_c \approx 155$ mm. The following plateau region is caused by the decreasing throat area (figure 4, bottom left). Finally the bottom right image shows the sign of the area trend: a positive value indicates an area increase; a negative value indicates an area decrease. Thus, up to a cone location of $x_c \approx 125$ mm the intake

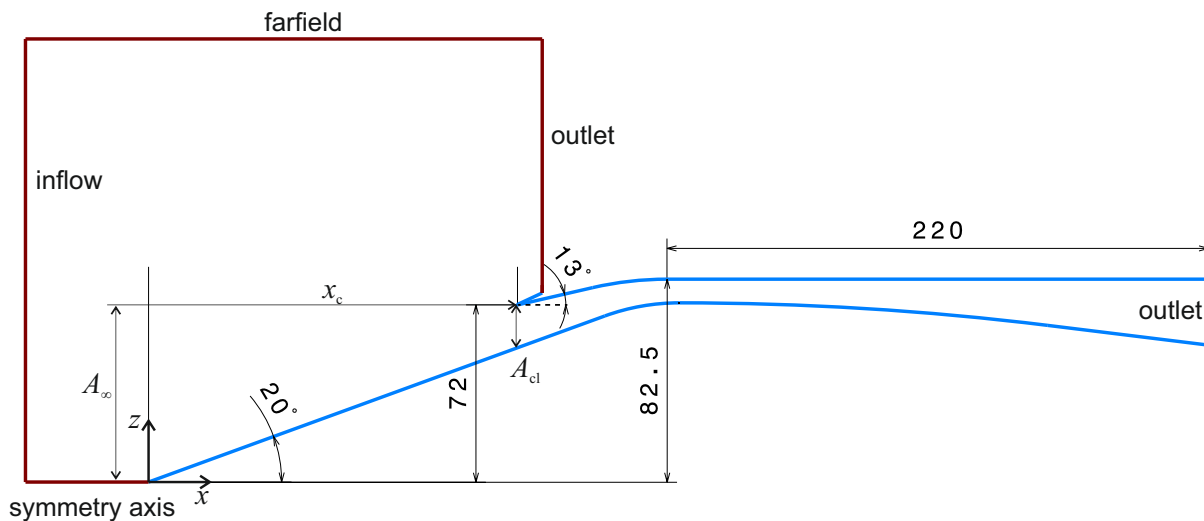


Fig 3. Sketch of the axisymmetric intake contour (blue line) and surrounding CFD domain.

has the unusual feature of having a diverging portion immediately downstream of its cowl. This is shown in figure 5, which contains two generic intake contours (red lines) and their cross sectional area distributions (blue lines).

2.2. Quasi Steady Approach

For the quasi steady approach, a numerical domain of an axisymmetric intake was designed for a fixed cone location and thus fixed internal contraction. The approach consisted of two batches of simulations. In each batch, multiple steady state simulations were performed successively, while the steady state solution of one simulation served as input for the successive one. In the first batch – the deceleration case – the Mach number was slowly decreased, while in the second batch – the acceleration case – the Mach number was slowly increased (see figure 6). During deceleration, the flow field was initiated with a relatively large Mach number, for example Mach 6 in the schematic case of figure 6 (a). The flow throughout the intake was started (i.e. fully developed) and successively the free stream Mach number was reduced with a sufficiently small step size. Once an intake unstart was observed, the step size of the Mach number decrease could be further refined to obtain more precise results for the detected unstart condition. During acceleration, the flow field was initiated with a relatively low Mach number, for example Mach 3 in the schematic case of figure 6 (b). For this low Mach number the flow throughout the intake was unstarted (i.e. there was mass spillage and subsonic flow through the intake) and successively the free stream Mach number was increased with a sufficiently small step size. Once the intake restart was observed, the step size of the Mach number increase could be further refined to obtain more precise results for the detected restart condition.

2.3. DLR-TAU Software System

The DLR-TAU software system was used to solve the Reynolds-Averaged Navier-Stokes (RANS) and Euler equations. DLR-TAU is a finite volume solver and explicit time stepping was used in this work. Furthermore, it was capable of parallelization to simultaneously run one simulation on multiple cores, thus absolute run times were reduced. For supersonic flow, inviscid terms were discretized with a second order upwind scheme, while second order central discretization was used for viscous terms. To faster damp out low frequency oscillations during time integration, the solver could be set to multigrid mode. Turbulence could be modeled with various models, such as one- or two-equation approaches. The $k - \omega$ Shear-Stress Transport (SST) model [11] was used throughout this work, because it proved to accurately model hypersonic intake flow fields [14, 2].

Table 1 lists the nominal free stream parameters of the different experiments. To this point, only TMK cases were duplicated numerically. In supersonic mode TMK operates at a total temperature

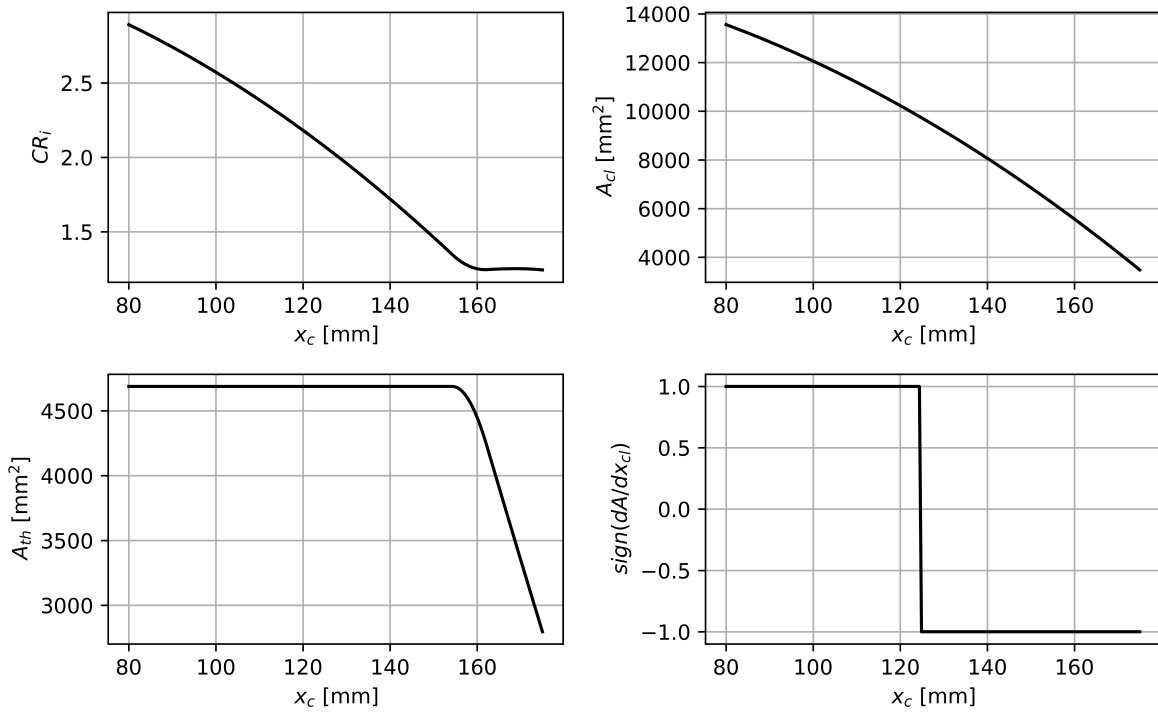


Fig 4. Configurational characteristics of axisymmetric intake.

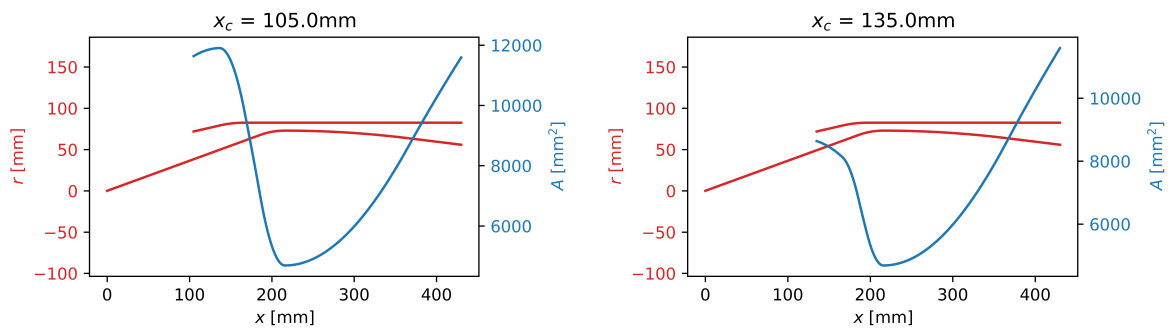


Fig 5. Generic intake configurations and cross-sectional area trend for cone located further downstream (left) and upstream (right).

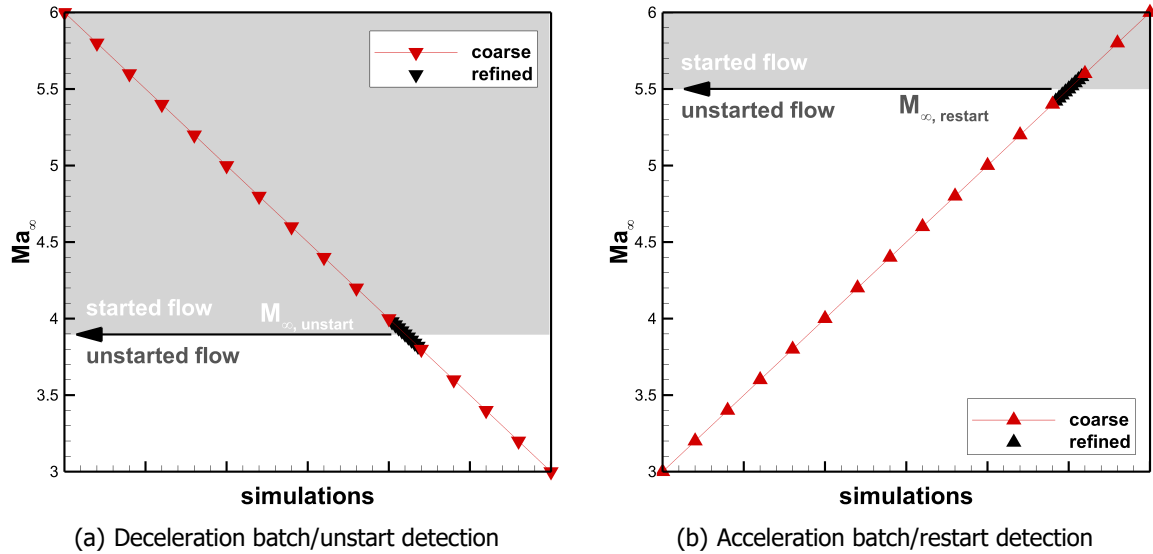


Fig 6. Schematic numerical procedure for detecting intake unstart and restart.

Table 1. Wind tunnel conditions.

Tunnel	M	Re Mio/m	T0 K	p0 bar	q bar
TMK	3.5	50.7	300	8.9	1
TMK	4	61	300	13.6	1
H2K	5.3	1.98	550	2.1	0.06
H2K	5.3	9.87	400	6.2	0.16

and dynamic pressure of 300 K and approximately 1 bar. Therefore, CFD conditions were set to the corresponding values. Wall temperature was treated as isothermal at $T_w = 300$ K.

3. Results

3.1. Comparison of Wall Pressure: CFD and Experiment

For a $M = 4$ reference case and a cone location of $x_c = 144.6$ mm, the steady state CFD solution was extensively cross-checked to the experimental data. In this context, a grid refinement study was performed, which can be found in [10, pp. 45], and is left out here due to brevity. Furthermore, the turbulence models were varied. Steady state wall pressures, measured during experiment, agreed well with results obtained from numerical simulations (see figure 7). Best results were obtained by the Menter SST model, which then was used for the quasi-steady approach.

3.2. Qualitative Discussion of CFD Flow Topology

To gain a better understanding of the intake flow, figure 8 shows density gradients extracted from CFD during deceleration and acceleration. For large Mach numbers, the conical shock hits underneath the cowl and causes reflections that march downstream. For the shock-on-lip case (2), there are still reflections at the cowl, but they appear to be weaker. During deceleration the intake remains started down to a Mach number of 3.1 and then unstarts when going to $M_\infty = 3.0$. In the unstarted flow field the flow topology near the cowl closure changes drastically. A large separation region and oblique shock are present and lead to a severe spillage across the intake cowl. For very low Mach numbers, such as $M_\infty = 2.0$, the strong shock moves upstream of the cowl's leading edge, even detaches, and causes large amounts of spillage mass flow.

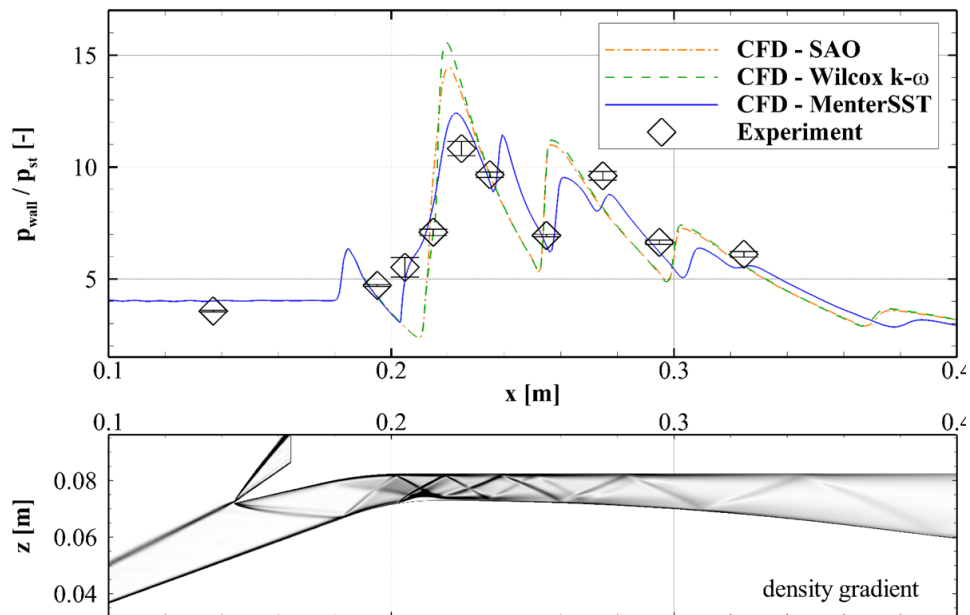


Fig 7. Experimental and numerical wall pressures on centerbody side of configuration for $M_\infty = 4$, $x_c = 144.6$ mm.

When accelerating the flow, the intake remains unstarted up to $M_\infty = 4.1$. For the two cases shown, i.e. (4) and (7), and (3) and (8), there are two physical solutions of the intake flow field. Complex flow structures, with large portions of subsonic flow are present in the internal portion of the intake. The intake finally restarts at $M_\infty = 4.2$. Thus, in the quasi steady approach, once the intake was unstarted due to the low Mach number, it had to re-accelerate from Mach 3 to 4.2 in order to restart.

3.3. Wind Tunnel Results

During the wind tunnel experiments, Mach number could not be varied, but was fixed at one condition. The movable cone, however, allowed for a change of internal contraction ratio during one wind tunnel run. With this, the internal contraction ratio could be varied, and the unstart and restart conditions could be detected. Figure 9 shows the critical internal contraction ratios for unstart (unfilled symbols) and restart (filled symbols), all plotted against the Mach number at the cowl closure. Mach number at the cowl closure was estimated as the mean of the Mach number immediately downstream of the conical shock and the final Mach number further downstream of the conical shock. For the $M_\infty = 5.3$ case, e.g., this corresponds to a value of $M_{cl} = 3.53$.

For the Mach 3.5 case, no unstart could be detected due to a malfunction of the translational-mechanism that moved the cone. The Mach 4 case showed large hysteresis effect, and after intake unstart the internal contraction had to be reduced by 0.34 to restart the intake. This corresponded to a cone displacement of 14 mm. The hysteresis effect in the Mach 5.3 was not as pronounced and turned out to be more severe for the large Reynolds number case, than for the low Reynolds number case. Note that the Mach 5.3 tests were performed in the hypersonic wind tunnel H2K, while the other tests were performed in the trisonic TMK wind tunnel. In this context, the empirical limit of Sun et al. [16] can be regarded as conservative for unstart prediction. The limits by Smart et al. [15] and Flock et al. [4] are slightly optimistic.

3.4. Comparison of Starting and Unstarting Conditions Extracted from CFD and Experiment

As mentioned already, the quasi-steady approach was applied to constant geometry configurations. The cone locations, at which an unstart or restart was detected experimentally, were used for the numerical simulations. Thus far, the quasi-steady approach was applied to three different cone locations. First,

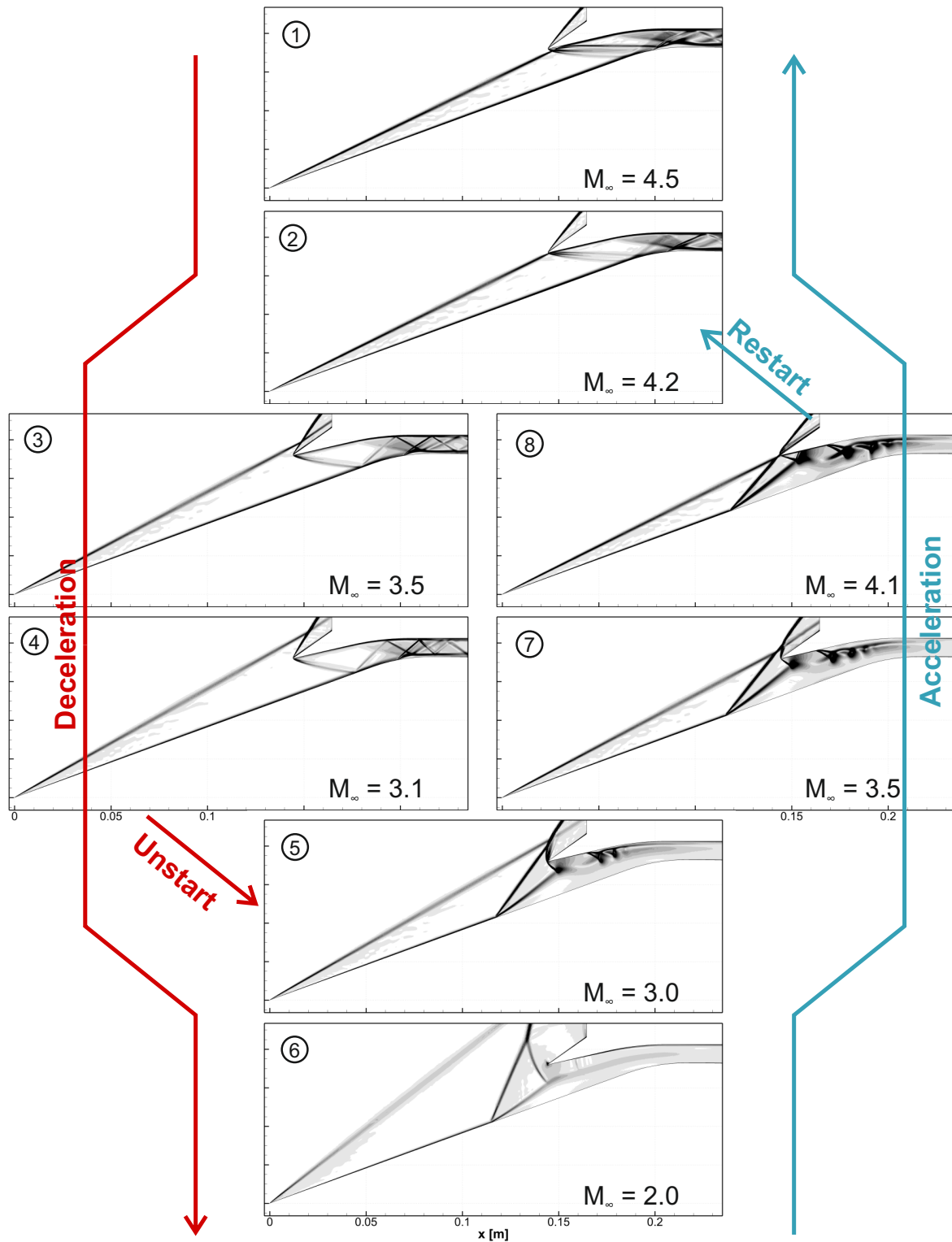


Fig 8. Density gradients extracted from CFD for various Mach numbers; $x_c = 144.5$ mm.

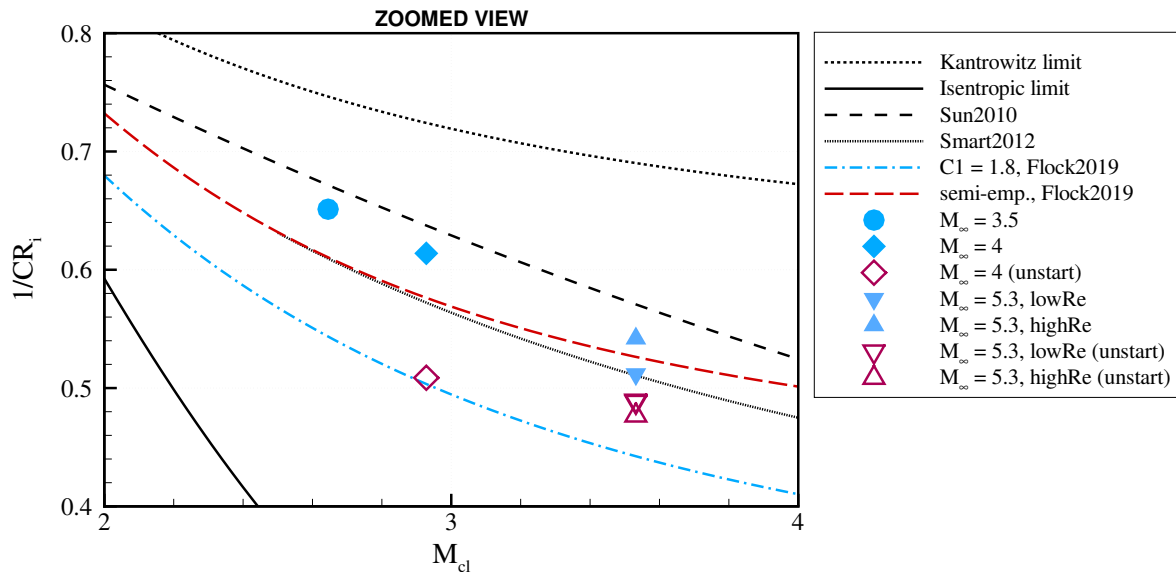


Fig 9. Kantrowitz diagram with experimental data of unstart (unfilled) and restart (filled) conditions.

to the $x_c = 130$ mm case, which is equivalent to $CR_i = 1.97$, $1/CR_i = 0.51$; second, to the $x_c = 144$ mm case, which is equivalent to $CR_i = 1.63$, $1/CR_i = 0.61$; third, to the $x_c = 148$ mm case, which is equivalent to $CR_i = 1.54$, $1/CR_i = 0.65$; For an ideal outcome, the intake configurations should restart or unstart at the same free stream Mach number, as the experiments were performed at.

Figure 10 shows a zoomed in view of the already discussed Kantrowitz diagram. The restart/unstart locations, which correspond to one another, are connected by black arrow-lines. The Mach 4 experiment is relatively well reproduced by the quasi steady approach, with a difference in Mach number of 3% and 7% for the restart and unstart/blockage case, respectively. For the Mach 3 case, only the restart case is reproduced with the quasi steady approach. The difference in restart Mach number of 5% is acceptable.

The collection of unstart and restart configuration is used to adjust the $C1$ factor (see , eq. (6) therein) for an unstart/blockage and restart limit, respectively. The empirical relation with $C1 = 1.43$ nicely reproduces the restart limit for the low Mach number cases. The high Mach number cases (i.e. $M_\infty = 5.3$) restart at even larger internal contraction ratios. The empirical relations with $C1 = 1.71$ nicely reproduces the blockage limit over the entire range of Mach numbers.

4. Conclusion

In the present manuscript we described a quasi-steady, numerical approach to determine intake unstart and restart characteristics. An axisymmetric intake configuration with movable cone was used as reference configuration. Experimental results for unstart and restart, obtained in two supersonic wind tunnels are presented. The main findings include:

- The unstart and restart hysteresis, which is well known for supersonic intakes, was found during experiments and also during numerical simulations. It was more pronounced for lower Mach number.
- The unstart and restart Mach numbers from experiments could be detected to 7% by the quasi steady approach.
- The quasi-steady approach revealed insight into the internal flow field of the intake, especially during the hysteresis case.

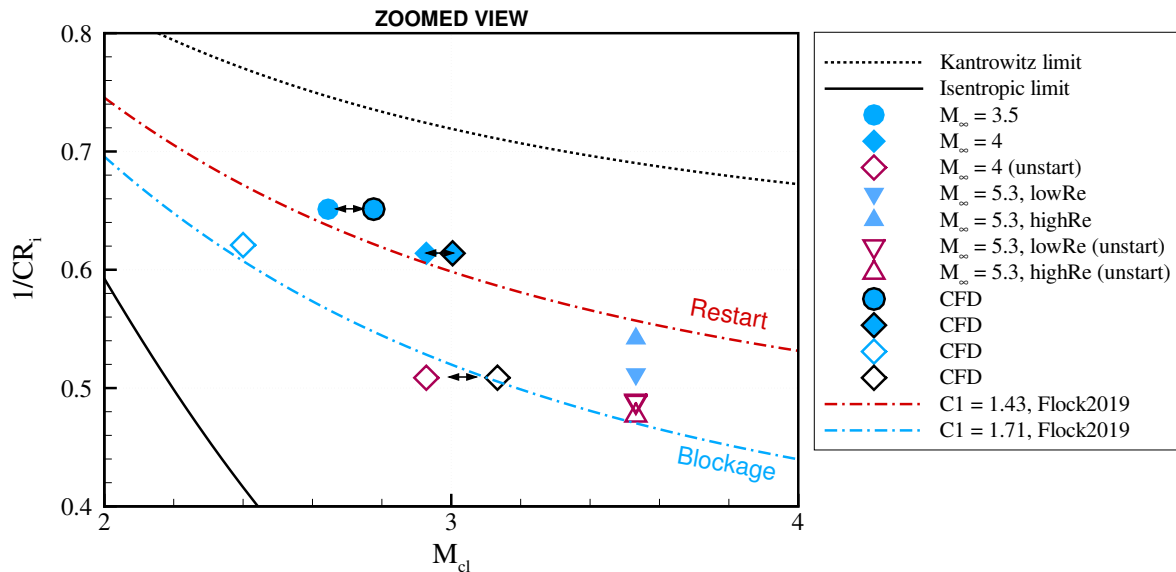


Fig 10. Kantrowitz diagram with comparison of experimental and numerical unstart and restart conditions.

- With an empirical relation, an unstart/blockage and restart limit could be detected, which can be used for further analysis of the axisymmetric intake configuration.

References

- [1] P Donde, A G Marathe, and K Sudhakar. Starting in Hypersonic Intakes. In *42nd AIAA/ASME/SAE/ASEE Joint Propulsion Conference & Exhibit*, number July, 2006.
- [2] Andreas K Flock and Ali Gülhan. Experimental and Numerical Performance Analysis of a Self Starting, Three-Dimensional SCRamjet Intake. In *20th AIAA International Space Planes and Hypersonic Systems and Technologies Conference*, number 2015-3680, Glasgow, 2015.
- [3] Andreas K Flock and Ali Gülhan. Experimental Investigation of the Starting Behavior of a Three-Dimensional Scramjet Intake. *AIAA Journal*, 53(9):2686–2693, 2015.
- [4] Andreas K. Flock and Ali Gülhan. Modified kantrowitz starting criteria for mixed compression supersonic intakes. *AIAA Journal*, 57(5):2011–2016, 2019.
- [5] A Grainger, S C Tirtrey, R R Boyce, S Paris, and G Paniagua. Starting Mechanisms for High Contraction Ratio Hypersonic Inlets. In *7th European Symposium on Aerothermodynamics*, 2011.
- [6] Lance S Jacobsen, Chung-Jen Tam, Robert Behdadnia, and Frederick S Billig. Starting and Operation of a Streamline-Traced Busemann Inlet at Mach 4. In *42nd AIAA/ASME/SAE/ASEE Joint Propulsion Conference & Exhibit*, number 2006-4508, pages 1–19, 2006.
- [7] M. K. Jain and S. Mittal. Euler flow in a supersonic mixed-compression inlet. *International Journal For Numerical Methods in Fluids*, 50:1405–1423, 2006.
- [8] Arthur Kantrowitz and Coleman duP. Donaldson. Preliminary Investigation of Supersonic Diffusers. *National Advisory Committee for Aeronautics*, 1945.
- [9] Sebastian Karl. *Numerical Investigation of a Generic Scramjet Configuration*. PhD thesis, Technical University Dresden, 2011.

- [10] Adrian TE Krieger. *Numerical Simulation of the Start and Unstart Behavior of a Ram- or Scramjet*. PhD thesis, RWTH Aachen, 2019.
- [11] F R Menter, M Kuntz, and R Langtry. Ten Years of Industrial Experience with the SST Turbulence Model. *Heat and Mass Transfer*, 4, 2003.
- [12] Hideaki Ogawa, Alexander L Grainger, and Russell R Boyce. Inlet Starting of High-Contraction Axisymmetric Scramjets. *Journal of Propulsion and Power*, 26(6):1247–1258, 2010.
- [13] K Oswatitsch. Pressure Recovery for Missiles with Reaction Propulsion at High Supersonic Speeds. *National Advisory Committee for Aeronautics*, 1944.
- [14] Johannes C Rieher. *Aerothermodynamische Analysis eines Scramjet-Flugexperiments*. f, RWTH Aachen, 2015.
- [15] Michael K Smart. How Much Compression Should a Scramjet Inlet Do? *AIAA Journal*, 50(3):610–619, 2012.
- [16] Bo Sun and Kun-Yuan Zhang. Empirical Equation for Self-Starting Limit of Supersonic Inlets. *Journal of Propulsion and Power*, 26(4), 2010.
- [17] Rabi Tahir, Sannu Molder, and Eugene Timofeev. Unsteady starting of high mach number air inlets – a cfd study. In *39th AIAA/ASME/SAE/ASEE Joint Propulsion Conference and Exhibit*, Reston, Virginia, 2003. American Institute of Aeronautics and Astronautics.
- [18] Evgeny V Timofeev, Rabi B Tahir, and Sannu Mölder. On Recent Developments Related to Flow Starting in Hypersonic Air Intakes. In *15th AIAA International Space Planes and Hypersonic Systems and Technologies Conference*, number 2008-2512, pages 1–9, 2008.